Bioorganic & Medicinal Chemistry Letters 27 (2017) 4056–4060

Contents lists available at ScienceDirect

Bioorganic & Medicinal Chemistry Letters

journal homepage: www.elsevier.com/locate/bmcl

Macrocyclic factor XIa inhibitors

Cailan Wang [a], James R. Corte [a], Karen A. Rossi [a], Jeffrey M. Bozarth [c], Yiming Wu [c], Steven Sheriff [b], Joseph E. Myers Jr. [b], Joseph M. Luettgen [c], Dietmar A. Seiffert [b], Ruth R. Wexler [a], Mimi L. Quan [a,*]

[a] Bristol-Myers Squibb Company, Research and Development, 350 Carter Road, Hopewell, NJ 08540 United States
[b] Bristol-Myers Squibb Company, Research and Development, US Rt. 206 & Province Line Road, Princeton, NJ 08540 United States
[c] Bristol-Myers Squibb Company, Research and Development, 311 Pennington-Rocky Hill Road, Pennington, NJ 08543-2130 United States

ARTICLE INFO

Article history:
Received 28 June 2017
Revised 13 July 2017
Accepted 19 July 2017
Available online 25 July 2017

Keywords:
Factor XIa inhibitors
FXIa
Activated partial thromboplastin time
aPTT
Thrombosis

ABSTRACT

A series of macrocyclic factor XIa (FXIa) inhibitors was designed based on an analysis of the crystal structures of the acyclic phenylimidazole compounds. Further optimization using structure-based design led to inhibitors with pM affinity for FXIa, excellent selectivity against a panel of relevant serine proteases, and good potency in the activated partial thromboplastin time (aPTT) clotting assay.

Thrombosis, the abnormal occlusion of a blood vessel which can lead to myocardial infarction and ischemic stroke is the leading cause of mortality and morbidity.[1] Approved thrombin and factor Xa (FXa) inhibitors[2] such as dabigatran, rivaroxaban, apixaban, and edoxaban are effective in the treatment and prevention of thrombosis. These novel oral anticoagulants (NOACs) have also addressed many issues related to warfarin.[3] However, there remains an unmet medical need for more efficacious medications with less bleeding risk.[4] Factor XIa is located upstream in the coagulation cascade and plays a major role in the amplification and propagation of thrombin production.[5] Genetic evidence indicates FXIa could be an antithrombotic target with an improved net clinical benefit.[6–8] Preclinical research has demonstrated that reversible FXIa inhibitors show robust efficacy with minimum bleeding in animal models.[9] This evidence suggests that inhibition of FXIa could be an effective means for preventing thrombosis with a reduced bleeding risk as compared to current therapies. Furthermore, a FXI-directed antisense oligonucleotide (ASO) has been shown to prevent thrombosis and appeared safe with respect to bleeding in a recent Phase II clinical trial.[10]

We have previously described a series of phenylimidazole FXIa inhibitors exemplified by compound **1** (Fig. 1).[11] To further enhance FXIa affinity, we sought to preorganize the bioactive conformation of **1** via a macrocyclization strategy. Recently we reported one of our macrocyclization approaches by removing the P1 prime phenyl and connecting the P1 prime to the ortho-position of the P2 prime phenyl via an alkyl linker (approach A in Fig. 1).[12] Herein, we describe another macrocyclization approach by linking the P1 prime phenyl directly to the P2 prime phenyl as shown by approach B in Fig. 1.

The FXIa bound X-ray structures of compound **1**[11c] and other related compounds showed that the binding conformation of the phenylimidazole-phenylalanine portion of the molecules are similar in most of the structures (Fig. 2). We envisioned based on proximity that the two phenyl groups could be linked as shown in Fig. 1 to form macrocycles that would pre-organize the inhibitor into its binding conformation and further improve its binding efficiency.

Various linkers connecting the meta- or para-position of the P1 prime phenyl to the ortho-position of the P2 prime phenyl were designed guided by modeling using the X-ray structure of **1**. The initial set of compounds with a 3-atom amide linker resulted in the *m*-linked compounds **4** and **5** being more potent than the *p*-linked analogs **6** and **7** (Table 1). The same trend was observed for compounds **8**–**10** with the 4-carbon linker. The *p*-linked connection altered the trajectory of the linker which contributed to a loss in FXIa affinity. Similar to the acyclic series, chloro-substitution at the 5-position of the imidazole improved FXIa affinity (see *m*-linked compounds **5** and **9**).[11a] The compounds with the 4-atom alkyl linker were more potent than the compounds with the 3-atom amide linker. Molecular modeling suggested the

* Corresponding author.
E-mail address: mimi.quan@bms.com (M.L. Quan).

http://dx.doi.org/10.1016/j.bmcl.2017.07.048
0960-894X/

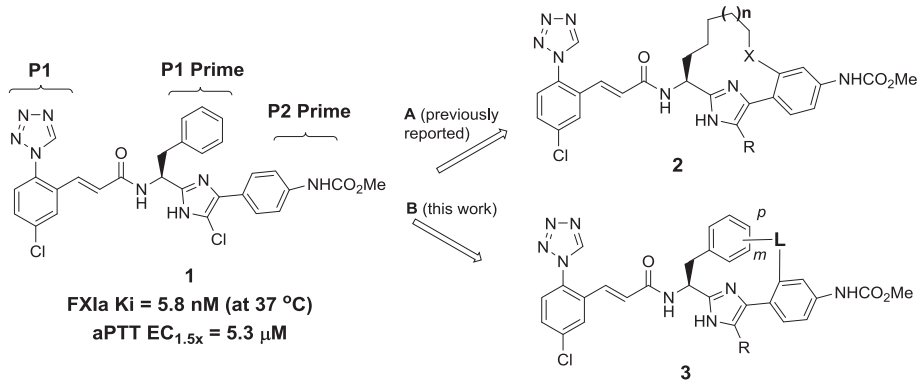

Fig. 1. From acyclic to macrocycle FXIa inhibitors.

Table 1
Initial macrocycles.

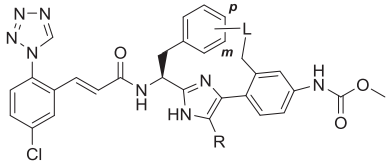

Compd	L	Ring size	R	FXIa Ki[a] (nM)
4	*m*-CONH	13	H	500
5	*m*-CONH	13	Cl	92
6	*p*-CONH	14	H	6400
7	*p*-CONH	14	Cl	8100
8	*m*-$(CH_2)_3$	14	H	17
9	***m*-$(CH_2)_3$**	**14**	**Cl**	**8.2**
10	*p*-$(CH_2)_3$	15	H	71

[a] Ki values were obtained from purified human enzyme and a synthetic peptides substrate at 25 °C and were averaged from multiple determinations (n = 2), as described in Ref. 13.

conformation of the macrocycle with the 3-atom amide linker was strained. The 14-membered ring macrocycle containing the longer linker alleviated the strain thus leading to improved FXIa affinity. The human plasma concentration of FXIa inhibitor which produced an increase of 50% over the baseline in activated partial thromboplastin time ($aPTT_{1.5x}$) was used to assess the in vitro anticoagulant activity. Compound **9** achieved single digit nanomolar affinity for FXIa with moderate in vitro anticoagulant activity ($aPTT_{1.5x}$ = 34 μM).

Modeling suggested that the overall binding mode for macrocycle **9** was similar to acyclic phenylimidazole **1** (Fig. 2) and further indicated the possibility to form a hydrogen bond with the carbonyl of Leu41 with an NH moiety in the linker, similar to our alkyl linked macrocycles previously reported.[12] Therefore the amide linker was incorporated in compound **11** resulting in an approximate 10-fold improvement in both the FXIa affinity and in vitro anticoagulant activity (aPTT) compared to **8** (Table 2). Initial molecular modeling also suggested that incorporation of substitution at the para-position of the P1 prime phenyl ring could interact with the Cys42-Cys58 disulfide bridge to further improve binding affinity. Indeed, fluorine-analog **12** enhanced FXIa affinity by 3-fold and achieved subnanomolar affinity. Replacement of the P1 prime phenyl ring with a pyridine led to compound **13** with 5-fold improvement in both FXIa affinity and in vitro anticoagulant activity (aPTT)

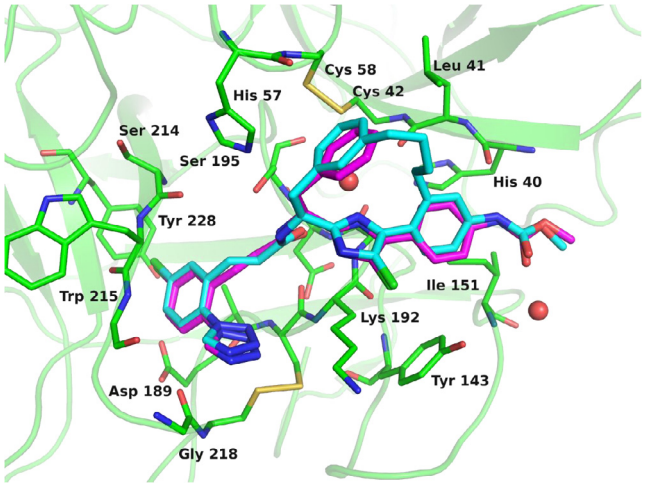

Fig. 2. Superposition of crystal structure of **1** (in purple) and model of **9** (in cyan).

compared to **11**. Further SAR efforts to incorporate both modifications into one molecule resulted in compound **14** with picomolar FXIa affinity (FXIa Ki = 0.02 nM). Compound **14** is highly selective

Table 2
Linker optimization of the 14-macrocycles.

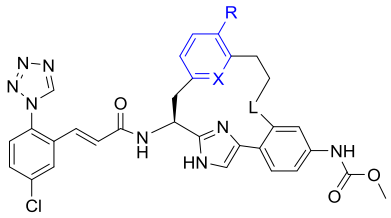

Compd	R/X	L	FXIa Ki[a] (nM)	aPTT[b]$_{1.5x}$ (μM)
8	H/CH	CH_2CH_2	17	23
11	H/CH	C(O)NH	1.5	2.1
12	F/CH	C(O)NH	0.53	1.4
13	H/N	C(O)NH	0.32	0.40
14	**F/N**	**C(O)NH**	**0.02**	**0.27**

[a] Ki values were obtained from purified human enzyme and a synthetic peptide substrate at 37 °C (except for **8** at 25 °C) and were averaged from multiple determinations (n = 2), as described in Ref. 13.
[b] aPTT (activated partial thromboplastin time) in vitro clotting assay was performed in human plasma.

over a panel of relevant serine proteases (Trypsin Ki = 670 nM, FVIIa Ki = 1100 nM, FXa Ki = 1400 nM, FIIa Ki > 13,000 nM). The in vitro anticoagulant activity was also slightly improved compared to **13** (aPTT$_{1.5x}$ = 0.27 μM, Table 2). Importantly, comparing macrocycle **14** with acyclic phenylimidazole **1**, the macrocyclic analog improved FXIa affinity by 290-fold and aPTT potency by 19-fold.

An X-ray structure of **14** in the FXIa active site was obtained (Fig. 3A, 2.35 Å, PBD ID = 5W86). The general binding mode is similar to **1**. A hydrogen bond is observed between the NH of the amide with the carbonyl of Leu41 as designed. Interestingly, the fluorine makes van der Waals contact with Tyr58b C(α) instead of interacting with the Cys42-Cys58 disulfide bridge as initially anticipated based on the design (Fig. 3B). The difference in potency between **12** and **14** can be rationalized by examining the ligand strain. The macrocycle in general is a highly strained system and almost all atoms have intramolecular van der Waals contact. By replacing the phenyl in **12** with a pyridine in **14**, some of the ligand strain is reduced, possibly contributing to the improvement in potency. Conformational analysis on the macrocycles supports this theory in that twice as many conformations were observed for **14** compared to **12**.

Synthesis of the macrocycles with a 3-atom amide linker is exemplified in Scheme 1. Condensation of bromomethylketone **15**[12] with Boc-L-phenylalanine **16** followed by imidazole formation gave phenylimidazole **17**. Compound **17** was treated with zinc (II) cyanide under microwave radiation to give **18**. Saponification of **18** followed by hydrogenation afforded **19**. Macrolactamization of **19** under dilute conditions with BOP and DMAP, followed by Boc deprotection, provided macrocycle **20**. Amide coupling of **20** with *N*-hydroxysuccinate ester **21**[11b] produced compound **4**. Chlorination of **4** afforded chloroimidazole analog **5**.

The synthesis of the macrocycles with a 4-carbon linker is illustrated by the preparation of compounds **8** and **9** (Scheme 2). Compound **23**, prepared from **15** and **22** as described previously, reacted with SEMCl to generate **24**. Suzuki coupling of **24** with 2-allyl-4,4,5,5-tetramethyl-1,3,2-dioxaborolane afforded **25**. Metathesis of **25** using 2nd generation Grubbs catalyst in the presence of *p*TsOH and high dilution conditions yielded macrocycle **26** as a mixture of *E* and *Z* isomers. Hydrogenation of **26**, followed by

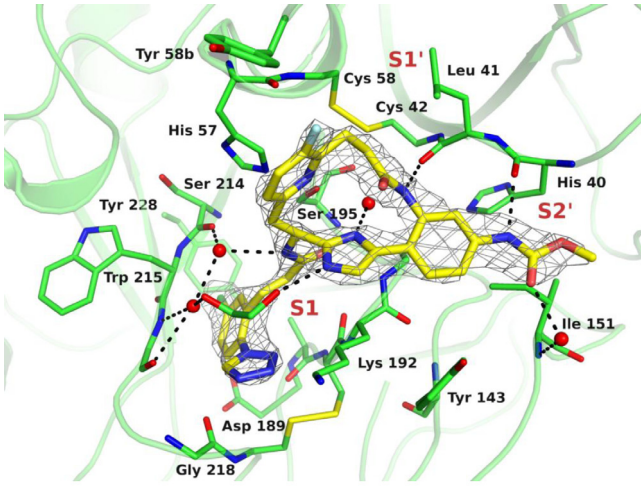

(A)

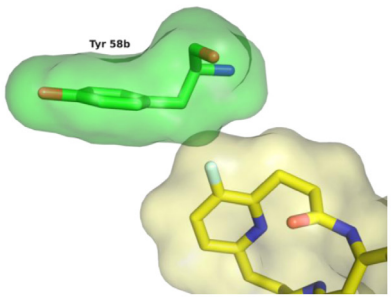

(B)

Fig. 3. (A) X-ray crystal structure of **14** bound in the active site of FXIa with omit electron density (gray mesh). The red spheres depict water molecules, the dotted lines depict hydrogen bonds, and ethylene diol is an artifact of the flash-cooling procedure. (B) van der Waals contact between Tyr58b C(α) and the fluorine on the pyridine ring.

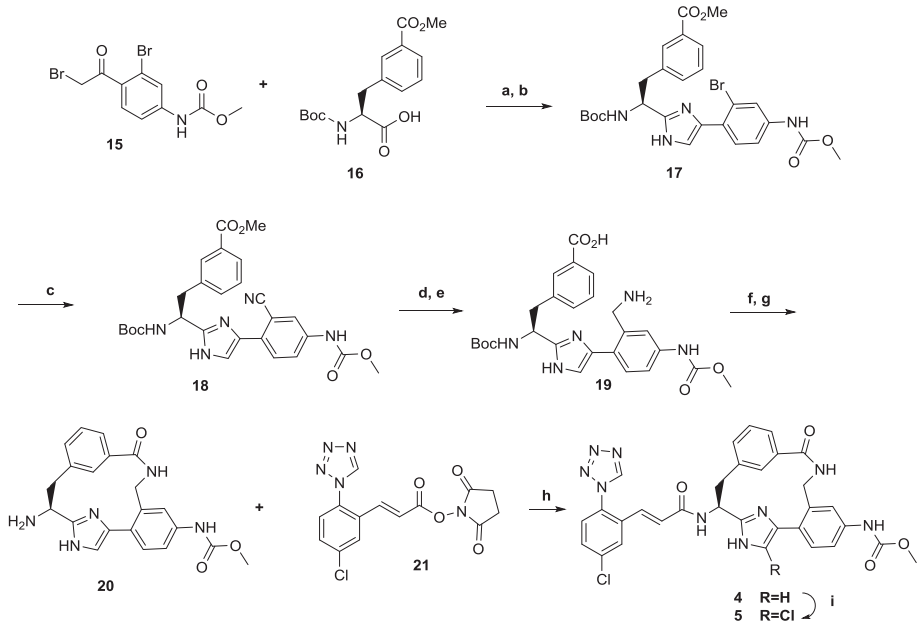

Scheme 1. Reagents and conditions: (a) $KHCO_3$, DMF, 0 °C to rt; (b) NH_4OAc, xylene, reflux (Dean-Stark trap), 3 h, 53% over two steps; (c) $Zn(CN)_2$, $Pd(PPh_3)_4$, DMF, 140 °C, microwave, 65%; (d) LiOH, THF/water, 100%; (e) Raney Ni, H_2, water-NH_4OH (2:1), 90%; (f) BOP, DMAP, DIEA, DMF/DCM, syringe pump slow addition, 90%; (g) TFA/DCM; (h) DIEA, DMF, 43% over two steps; (i) NCS, MeCN, TEA, 0–10 °C, 42%.

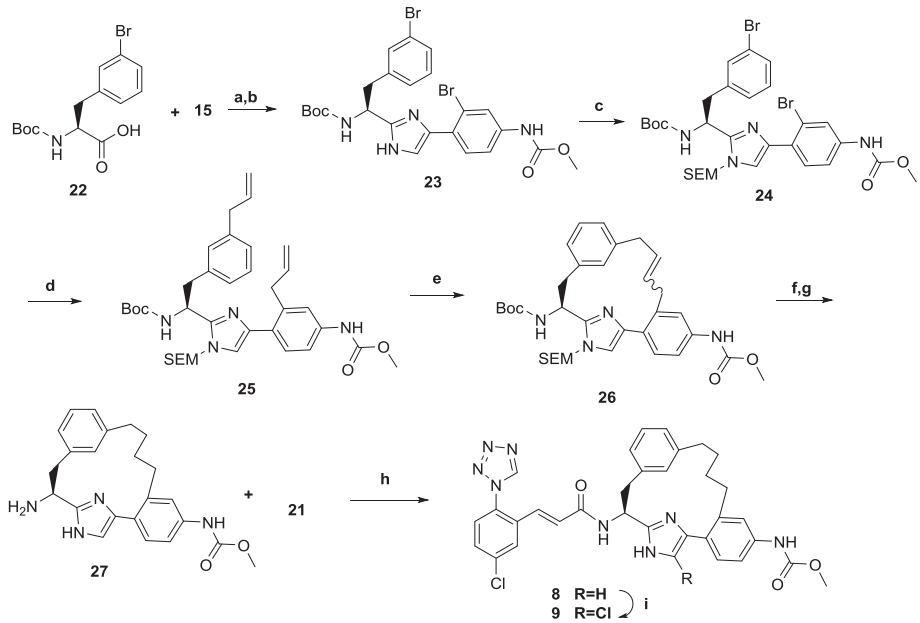

Scheme 2. Reagents and conditions: (a) $KHCO_3$, DMF, 0 °C to rt; (b) NH_4OAc, xylene, reflux (Dean-Stark), 3 h, 45% over two steps; (c) NaH, THF, SEMCl, 78%; (d) 2-allyl-4,4,5,5-tetramethyl-1,3,2-dioxaborolane, $Pd(dppf)Cl_2$, K_2CO_3, THF, 80 °C, 16 h, 31%; (e) *p*TsOH, DCM (1 mM), reflux, 2nd generation Grubbs catalyst, 34%; (f) H_2, Pd/C, MeOH, 91%; (g) 5 M HCl (aq), MeOH, 75 °C, 4 h, 90%; (h) DIEA, DMF, 38%; (i) NCS, MeCN, DIEA, 0–5 °C, 67%.

removal of the Boc and SEM groups, afforded amine **27**. Amide formation provided compound **8**, and chlorination of **8** yielded compound **9**.

Compound **14** was prepared as outlined in Scheme 3. 4-Iodo-3-nitroaniline (**28**) was converted to methylcarbamate **29** with methylchloroformate. Reaction of **29** with tributyl(1-ethoxyvinyl) stannane afforded **30**. Bromination of **30** with NBS gave bromomethylketone **31**. 2-Bromo-3-fluoro-6-methylpyridine (**32**) was brominated with NBS to give benzyl bromide **33**. Treatment of **33** and diethyl 2-acetamidomalonate with NaH afforded **34**. Hydrolysis followed by decarboxylation afforded an amino acid intermediate, which was protected with Boc anhydride to yield **35**. Reaction of **35** with **31** followed by imidazole formation as described previously resulted in **36**. Compound **36** was coupled with methyl acrylate to give **37**. Hydrogenation and saponification, followed by BOP-mediated macrolactamization under dilute conditions provided macrocycle **38**. Boc deprotection and subsequent amide formation, followed by chiral separation afforded **14**.

In summary, we have successfully designed and optimized a series of macrocycles with high FXIa affinity and excellent selectivity using structure-based drug design. Compound **14** achieved picomolar FXIa affinity and potent in vitro anticoagulant activity.

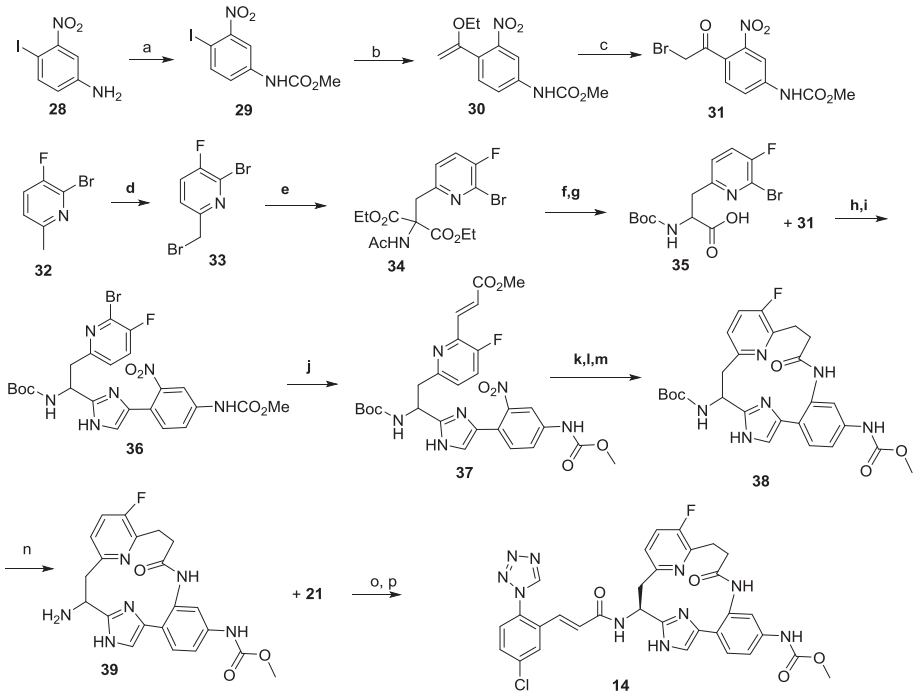

Scheme 3. Reagents and conditions: (a) Methyl chloroformate, pyridine, DCM, 96%; (b) Tributyl(1-ethoxyvinyl) stannane, $PdCl_2(PPh_3)_2$, PhMe, reflux, 58%; (c) NBS, THF/water, 99%; (d) NBS/AIBN, CCl_4, reflux; (e) diethyl 2-acetamidomalonate, NaH, DMF, 50% over two steps; (f) HCl (6 N aq.), dioxane, reflux; (g) $(Boc)_2O$, NaOH (1 N aq.), dioxane, 88% over two steps; (h) $KHCO_3$, DMF, 0 °C to rt, 77%; (i) NH_4OAc, xylene, reflux (Dean-Stark), 3 h, 12%; (j) methyl acrylate, $Pd(OAc)_2$, tri-tolyphosphine, DIEA, MeCN, microwave, 7–10%; (k) H_2, Pd/C, EtOAc/MeOH, 99%; (l) LiOH, THF/water, 95%; (m) BOP, DMAP, DIEA, DMF/DCM, syringe pump slow addition, 72%; (n) TFA/DCM; (o) DIEA, DMF, 0 °C to rt, 64% over two steps; (p) Chiral HPLC separation: Chiralcel OD-H, 70% (1:1 MeOH/EtOH with 0.1% DEA in heptane).

The potent FXIa affinity of these compounds enables further optimization of other parameters to achieve oral bioavailability which will be reported in due course.

Acknowledgments

The authors thank the Department of Discovery Synthesis for the synthesis of intermediates at BMS Biocon Research Center and the Department of Lead Discovery & Optimization for in vitro work.

A. Supplementary data

Supplementary data associated with this article can be found, in the online version, at http://dx.doi.org/10.1016/j.bmcl.2017.07.048.

References

1. Reddy KS. *Lancet*. 2016;388:1459–1544.
2. (a) Morais J, De Caterina R. *Cardiovasc Drugs Ther*. 2016;30:201–214;
   (b) Schaefer JK, McBane RD, Wysokinski WE. *Ann Hematol*. 2016;95:437–449;
   (c) Levy JH, Spyropoulos AC, Samama CM, Douketis JJ. *Am Coll Cardiol Intv*. 2014;7:1333–1351.
3. (a) Ansell J, Hirsh J, Hylek E, Jacobson A, Crowther M, Palareti G. *Chest*. 2008;133:160S–198S;
   (b) Stein PD, Grandison D, Hua TA. *Postgrad Med J*. 1994;70:S72–S83;
   (b) Hirsh J, Poller L. *Arch Int Med*. 1994;154:282–288.
4. (a) Sharma M, Cornelius VR, Patel JP, Davies JG, Molokhia M. *Circulation*. 2015;132:194–204;
   (b) Ruff CT, Giugliano RP, Braunwald E, et al. *Lancet*. 2014;383:955–962.
5. (a) Emsley J, McEwan PA, Gailani D. *Blood*. 2010;115:2569–2577;
   (b) Gailani D, Renne T. *Arterioscler Thromb Vasc Biol*. 2007;27:2507–2513;
   (c) von dem Borne PA, Meijers JCM, Bouma BN. *Blood*. 1995;86:3035–3042.
6. Bane CE, Neff AT, Gailani D. Factor XI deficiency or hemophilia C. In: Saba HI, Roberts HR, eds. *Hemostasis and Thrombosis: Practical Guidelines in Clinical Management*. Oxford: John Wiley & Sons Ltd; 2014:71–81.
7. (a) Salomon O, Steinberg DM, Koren-Morag N, Tanne D, Seligsohn U. *Blood*. 2008;111:4113–4117;
   (b) Salomon O, Steinberg DM, Dardik R, et al. *J Thromb Haemost*. 2003;1:658–661;
   (c) Salomon O, Steinberg DM, Zucker M, Varon D, Zivelin A, Seligsohn U. *Thromb Haemost*. 2011;105:269–273.
8. (a) Doggen CJM, Rosendaal FR, Meijers JCM. *Blood*. 2006;108:4045–4051;
   (b) Meijers JCM, Tekelenburg WLH, Bouma BN, Bertina RM, Rosendaal FR. *N Engl J Med*. 2000;342:696–701.
9. Wong PC, Quan ML, Watson CA, et al. *Thromb Thrombolysis*. 2015;40:416–423.
10. Buller HR, Bethune C, Bhanot S, et al. *N Engl J Med*. 2015;372:232–240.
11. (a) Hangeland JJ, Friends TJ, Rossi KA, et al. *J Med Chem*. 2014;57:9915;
   (b) Pinto DJ, Smallheer JM, Corte JR, et al. *Bioorg Med Chem Lett*. 2015;25:1635;
   (c) Hu Z, Wong PC, Gilligan PJ, et al. *ACS Med Chem Lett*. 2015;6:590–595.
12. Corte JR, Fang T, Osuna H, et al. *J Med Chem*. 2017;60:1060–1075.
13. Quan ML, Wong PC, Wang C, et al. *J Med Chem*. 2014;57:955–969.